# POST-EPS COMPETING SCATTEROMETER DESIGNS: ASCAT VERSUS RFSCAT

**Georg Egger[(1)], Maria Belmonte Rivas[(2)]**

*[(1)] EADS Astrium GmbH, 88039 Friedrichshafen, Germany, georg.egger@astrium.eads.net*
*[(2)] Royal Netherlands Meteorological Institute (KNMI), Wilhelminalaan 10, 3732GK De Bilt, Netherlands, belmonte@knmi.nl*

## INTRODUCTION

Post–EPS is the successor of the EUMETSAT Polar System (EPS) and will provide continuity of operation for a range of polar orbiting Earth observation missions, among which the determination of ocean winds with scatterometry (SCA) ranks high in priority. Scatterometry presently enjoys a strong heritage: the ASCAT instrument onboard MetOp continues the series of European C-band fixed fan-beam scatterometers that started with the ERS-1 and ERS-2 satellites, whereas the American SeaWinds instrument operates in Ku-band with a rotating pencil-beam antenna. A preliminary study defining and analysing the novel rotating fan-beam RFSCAT concept was put forward in 2000 [1] [2]. For Post–EPS a trade-off between these scatterometer concepts has been carried out that includes technical, programmatical and most prominently end-to-end user considerations. This paper focuses on an objective performance comparison between RFSCAT configurations with different rotational speeds and the ASCAT baseline configuration.

## ASCAT AND RFSCAT CONCEPTS

To address the demands for improved swath coverage, spatial resolution and radiometric properties of the next generation of European scatterometers, two concepts have been selected as candidates for the follow-on Post-EPS:

- The ASCAT concept: It maintains most of the features inherited from the ASCAT on MetOp, like 6 fixed, 45 degrees spaced fan-beams and a long pulse measurement principle.
- The RFSCAT concept: Consists of a (or more) rotating fan-beam(s), e.g. a rotating ASCAT mid-antenna. Due to the larger footprint the rotation speed of the antenna may be much lower than for SeaWinds.

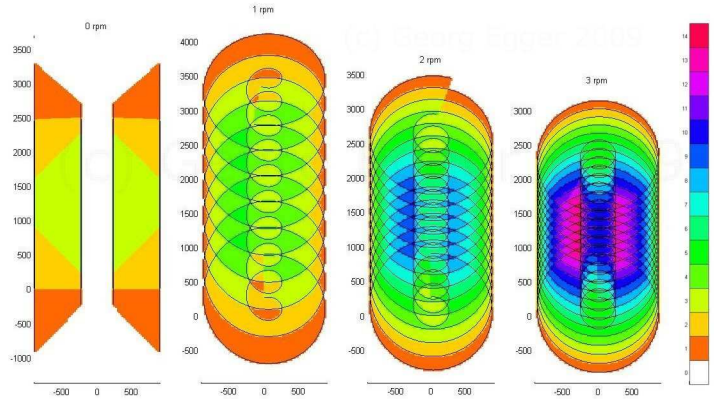


Fig. 1. ASCAT and RFSCAT acquisitions with 1, 2, and 3 rpm scan. The number of views is exactly 3 for ASCAT, meanwhile f it varies along and across the swath for RFSCAT.

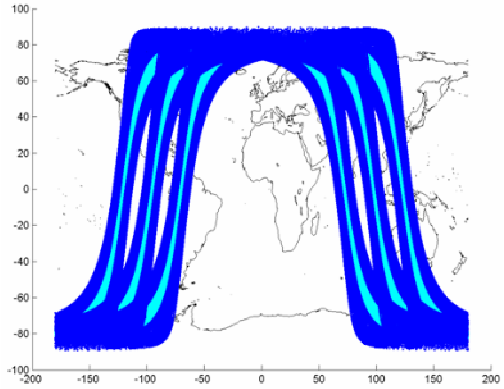

Fig. 2. The supposedly improved ground coverage of the RFSCAT (cyan) compared to the dual-swath with nadir gap of ASCAT.

### Measurement geometry

Crucial for optimal wind retrieval performance are accurate backscatter measurements collected from a diversity of azimuth angles. While the ASCAT concept provides a fixed number of azimuth views per cell across the swath from the fore, mid and aft beams, the acquisition geometry of the RFSCAT concept varies strongly across the swath and depends on the antenna rotation rate, as illustrated in Fig. 1. In order to ensure comparability, the same incidence angle range is chosen for RFSCAT and ASCAT. The RFSCAT antenna can be considered identical to the ASCAT mid-beam. In order to improve coverage, it was chosen to select the mid-beam incidence angle range from 20.0 (minimum allowed) to 53.5 degrees (ASCAT heritage value), the incidence angle range for the side-beams follow. A shaped gain pattern partially compensates the variations in SNR due to the slant range variations. The spatial resolution requirement determines the length of the antennas.

### Observational requirements summary

The requirements of the proposed configurations meets the Post-EPS requirements, mainly regarding spatial resolution (25 km), dynamic range (from 4 to 25 m/s), radiometric resolution (3% with relaxations up to 10% for low winds) and coverage (about global coverage within 48 hours). C-band has been selected as operating frequency because of its robustness against rain and atmospheric attenuation, and its higher saturation level for extreme winds.

**Timing scheme and radar waveform**

Two different timing schemes may be used for SCA:

- Short pulse: A scatterometer can be seen as a real-aperture radar, and it is feasible to assume a classical approach with short pulses and a high pulse repetition rate (PRF), as the number of looks of a measurement cell shall be maximised. The Doppler shift causes a location-dependent frequency offset of the echo signal, which can be effectively pre-compensated only for pencil beams. The major drawbacks of this timing scheme are the inter-pulse interferences and impaired noise measurements due to the presence of echoes.
- Long pulse: On MetOp a new approach was implemented, which allows the use of a relatively low peak-power solid state amplifier. The chirped transmit pulse lasts until echoes from the whole swath are received and then the echoes from the whole swath are sampled and frequency transformed. After reception of the echo from the far end of the swath echoes from beyond may arrive, therefore the noise power measurements take place after the last echo from the horizon has arrived. Only then the next pulse is transmitted, leading to a low PRF. The beams are operated sequentially.

The long-pulse principle has the advantages of avoiding inter-pulse interference and of the clever way of measuring noise power in the absence of echoes, and shall therefore be preferred over the short-pulse timing. However, the rotation of the antenna and the associated azimuth scan loss impedes the use of long-pulse timing with the RFSCAT concept and it is better operated by short-pulse timing. Both the long- and short-pulse timings use linear frequency modulated chirps for range resolution at moderate peak power. The so called de-ramping process performs range resolution equivalent to a matched filter reception.

**Radiometric resolution**

Scatterometers usually have strict requirements on radiometric resolution $K_p$, which is determined by the number of signal looks per view $N_{Signal}$, the number of noise samples used for the noise power subtraction process $N_{Noise}$ and the single-look signal to noise ratio *SNR* (see e.g. [4]).

$$K_p^2 = \frac{\mathrm{var}\{\sigma^0\}}{\langle \sigma^0 \rangle^2} = \frac{1}{N_{Signal}}\left(1+\frac{1}{SNR}\right)^2 + \frac{1}{N_{Noise}}\left(\frac{1}{SNR}\right)^2 \quad (1)$$

Signal looks $N_{Signal}$ are achieved in azimuth and elevation domain. The number of looks in elevation can be chosen by the transmit chirp bandwidth and provides together with the transmit peak power some degree of freedom in the design of the scatterometer. In azimuth direction, the number of looks depends on the beam repetition frequency *BRF*, the ground velocity of the beam $v_{gnd}$ and the integration width, which corresponds with some margin to the horizontal resolution. The rotated beams of the RFSCAT concept sweep with a higher velocity over the ground than the fixed ASCAT beams. The number of noise samples is also concept dependent. For long-pulse timing, the scatterometer measures noise power without any interference from ground echoes. For short-pulse timing other ways of measuring noise in presence of echoes from ground need to be exploited. This may come at the expense of additional complexity and/or loss of signal looks.

**Proposed configurations**

For the RFSCAT concept a range of antenna rotation speeds are feasible. The RFSCAT study [2] suggests a rotation speed of about 3 rpm. Lower rotation speeds are valid, as long as continuous coverage of the swath is achieved, although an end-to-end performance metric is required in order to assess the impact of the scan rate on the overall performance. A number of configurations were designed according to Post-EPS requirements, an overview can be found in Tab. 1.

Tab. 1. Proposed configurations comparison

| **Concept type** | ASCAT 0 rpm | RFSCAT 1 rpm | RFSCAT 2 rpm | RFSCAT 3 rpm |
|---|---|---|---|---|
| **Tx duty cycle / PRF** | 29% / 29 Hz | 7% / 230 Hz | 7% / 230 Hz | 7% / 230 Hz |
| **HPA peak power** | 100% | 271% | 545% | 830% |
| **Instrument average power consumption** | 100% | 72% | 127% | 185% |

All configurations are technically feasible. Advantages of the RFSCAT concept include lower mass and potential lower power consumption. Between 1 and 2 rpm the RFSCAT concept is comparable in terms average power consumption to the ASCAT concept. The ASCAT benefits from in-orbit heritage, constant performance across and along the swath, well established and conservative measurement principle and compatibility to other instruments (no obstruction of field of views of other instruments on the Post-EPS platform).

**END-TO-END PERFORMANCE STUDY**

An objective comparison between scatterometer concepts is made difficult by their differing observation geometries. This section introduces a set of performance metrics that enable the evaluation of different concepts in terms of their output wind quality. The performance evaluation rests on the output wind statistics produced by an end-to-end wind retrieval simulator (see Fig. 3. ).

**Input to performance model**

Input to the wind retrieval simulator is the scatterometer configuration file, which describes the view geometry and radiometric noise properties of a backscatter vector per resolution cell across the swath. The scatterometer configuration file is generated by combining a simple orbital model with detailed system parameters that specify the arrangement of antennas, their radiation patterns, the radar chirp bandwidth, pulse repetition frequency and approach to noise estimation. The simulated backscatter measurements are calculated using the empirically derived Geophysical Model Function (GMF) for ocean backscatter at C-band (CMOD5) [4] for a given wind input sampled at observation angles prescribed in the configuration file and corrupted by additive Gaussian noise with a variance equal to the instrumental radiometric $K_p$ noise level defined in Eq.(1), and optionally geophysical noise.

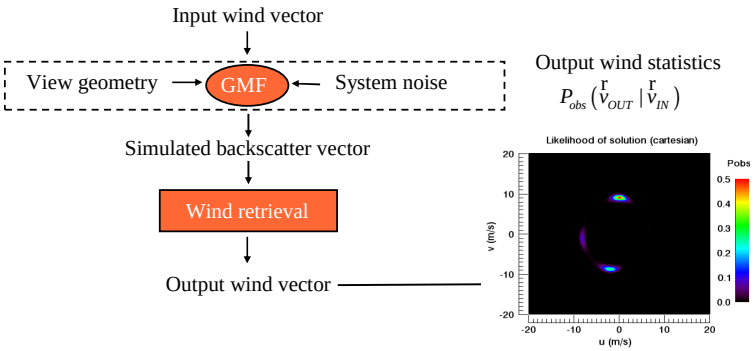


Fig. 3. End-to-end scatterometer performance model

**Wind retrieval and output wind statistics**

The wind retrieval procedure is based on a search for minimum squared distances between backscatter measurements $\sigma^0$ and backscatter model solutions $\sigma^0_{GMF}(u,v)$ lying on the GMF surface. The squared distance is defined as:

$$MLE(u,v) = \frac{1}{\langle MLE \rangle} \sum_{i=1,\ldots,N} \frac{\left|\sigma_i^0 - \sigma^0_{GMF,i}(u,v)\right|^2}{\mathrm{var}\{\sigma_i^0\}} \tag{2}$$

Where $N$ is the dimension of the backscatter vector (or the number of views), var$\{\sigma^0_i\}$ is the backscatter measurement variance for a particular view, and $<MLE>$ is an empirical normalization factor that accounts for deviations from the GMF caused by geophysical noise. If wind retrieval were a linear problem, then the distribution of wind outputs about the true wind input $P_{obs}(\mathbf{v}_{OUT}|\mathbf{v}_{IN})$ could be modeled as a chi-square distribution with 2 degrees of freedom (e.g. the dimensions of the GMF surface onto which noisy observation are projected):

$$P_{obs}(v_{out} \mid v_{in}) = \chi^2_{DoF=2}\left[MLE(v_{out} \mid v_{in})\right] \tag{3}$$

But the GMF surface bends and folds quite non-linearly in the space of measurements, whereby radiometric noise excursions in observations may cause wind solutions to land on nearby GMF branches, resulting in wind vector ambiguities and biases. A numerical Montecarlo approach with an end-to-end performance simulator is therefore recommended to generate statistical distributions of scatterometer wind outputs, such as the one displayed on the left panel in Fig. 4.

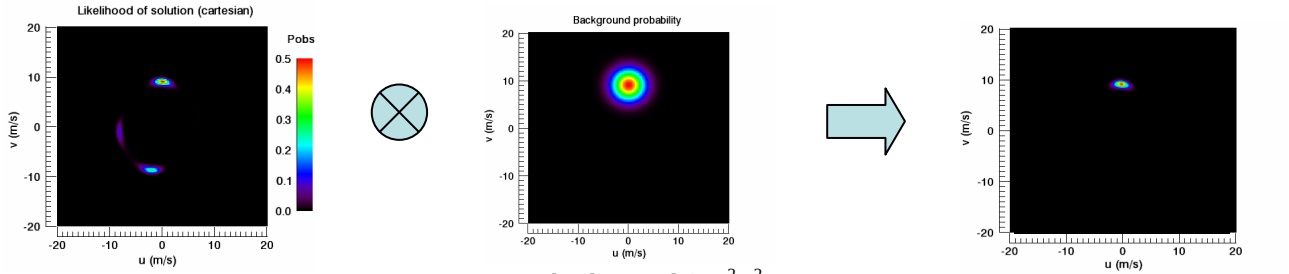


$P_{obs}(\mathbf{v}_{out}|\mathbf{v}_{in})$ NWP background ($5m^2/s^2$) $P_{obs}*P_{NWP}(\mathbf{v}_{out}|\mathbf{v}_{in})$

Fig. 4. Output wind (left), NWP background (mid) and background-constrained (right) wind statistics for an input wind of 9 m/s pointing along the y-axis.

The ambiguity removal approach currently used at KNMI draws from a priori NWP model background information and consists in minimizing a total cost function, whereby the first term contains the observational likelihood of a solution (i.e. the output wind statistics) and the second term contains a Gaussian probability distribution centered about a NWP wind forecast with 1D variance $\sigma_{NWP}{}^2 \sim 5\ m^2/s^2$, as illustrated on the middle panel in Fig. 4.

$$J = J_{obs} + J_{NWP} = -2\ln\left[P_{obs}(\vec{v}_{out} \mid \vec{v}_{in})\right] - 2\ln\left[P_{NWP}(\vec{v}_{out} \mid \vec{v}_{in})\right] \tag{4}$$

**Wind performance metrics**

To characterize the quality of a wind output, three separate figures of merit are introduced:

1. The *susceptibility to ambiguity* quantifies the reliance of the scatterometer wind retrievals on NWP background information and should be as low as possible:

$$FoM_{amb}(\vec{v}_{in}) = \int P_{obs}(\vec{v}_{out} \mid \vec{v}_{in}) - P_{obs} \cdot P_{NWP}(\vec{v}_{out} \mid \vec{v}_{in}) d^2 v_{out} \tag{5}$$

2. The *wind vector RMS error* quantifies the total wind retrieval error after ambiguity removal and should be as low as possible:

$$FoM(\vec{v}_{in}) = \sqrt{\int |\vec{v}_{out} - \vec{v}_{in}|^2 \cdot P_{obs} \cdot P_{NWP}(\vec{v}_{out} \mid \vec{v}_{in}) \, d^2 v_{out} / 2\sigma_{NWP}^2} \tag{6}$$

3. The *directional bias* quantifies the output wind directional bias after ambiguity removal and should be as low as possible:

$$dirbias(\vec{v}_{in}) = |\vec{v}_{in}| \int (\phi_{in} - \phi_{out}) \cdot P_{obs} \cdot P_{NWP}(\vec{v}_{out} \mid \vec{v}_{in}) \, d\phi_{out} \tag{7}$$

Wind retrieval is a nonlinear problem and the output wind statistics remain dependent on wind input. This issue is overcome by averaging the calculated performance metrics over a climatology of wind inputs with uniformly distributed directions and wind speeds following a Weibull distribution with a maximum around 9 m/s. The resulting performance metrics for the selected Post-EPS fixed beam ASCAT and rotating fan beam RFSCAT concepts are shown in Fig. 5.

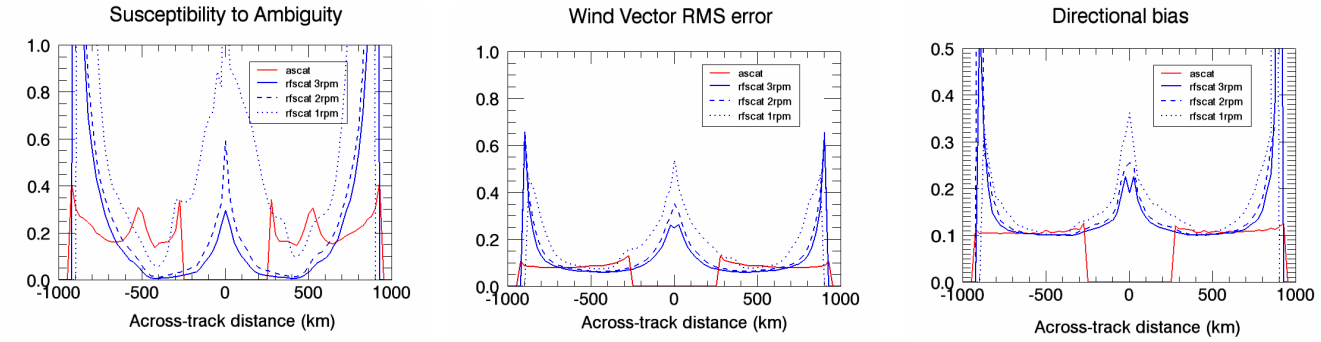


Fig. 5. Scatterometer performance metrics: Calculated directional bias and observed accumulation of wind solutions for SeaWinds at low wind speeds.

## SUMMARY AND CONCLUSIONS

An homogeneous attempt to objective end-to-end wind retrieval performance for different scatterometer configurations has been carried out for the first time. The results reveal and quantify the intrinsic properties of the different proposed concepts. In line with the observation geometry of acquired views, the wind retrieval performance of the ASCAT concept is quite uniform across the swath, while the RFSCAT wind retrieval performance depends strongly on across-track location and degrades significantly at nadir and the swath edges. Little difference can be seen in the usable swath width of the concepts: even though the RFSCAT concept has a much larger swath width (almost 2000 km), large parts of it do not reach competitive performance. All three performance metrics (wind ambiguity, RMS error and bias) show that the RFSCAT configurations are equal or superior to the ASCAT until about 650 km. Then the ASCAT concept takes the lead (until about 950 km). The usable single sided swath width of both fixed and rotating beam concepts is. For a fair comparison of the concepts, configurations with about equal power consumption shall be chosen. The ASCAT concept shall therefore be compared with an RFSCAT with a scan rate between 1 and 2 rpm.

**Funding**

The work leading to this publication was carried out under an ESA contract with reference ITT number AO 1-5351/07/NL/EL, ESA/IPC(2006)11, rev.17, item no. 06.155.05, budget output 100631 EOPA.

## REFERENCES

[1] C.C. Lin, B. Rommen, J.J.W.Wilson, F. Impagnatiello, P.S.Park, “An Analysis of a rotating, range-gated, fanbeam spaceborne scatterometer concept”, IEEE Trans. Geosc. Rem. Sens., Vol.38, No.5, 2000.

[2] C.C. Lin, A. Stoffelen, J. de Kloe, V. Wismann, S. Bartha, H.-R. Schulte: Wind retrieval capability of rotating, range-gated, fanbeam spaceborne scatterometer, Proc. SPIE, Vol. 4881, 268 (2003); doi:10.1117/12.462995

[3] H. Hersbach, A. Stoffelen and S. de Haan, “An Improved C-band scatterometer ocean geophysical model function: CMOD5”, J. Geophys. Res., 112, 2007.

[4] M.W. Spencer, C. Wu, D.G. Long, “Improved resolution backscatter measurements with the SeaWinds Pencil-Beam Scatterometer”, IEEE TGRS, 38(1), 2000.